J. Physiol. (1979), **291**, *pp.* 507–530
With 13 *text-figures*
Printed in Great Britain

INACTIVATION OF DELAYED OUTWARD CURRENT IN MOLLUSCAN NEURONE SOMATA

BY R. W. ALDRICH JR.*, P. A. GETTING AND S. H. THOMPSON*
From the Department of Biological Sciences, Stanford University, Stanford, California 94305, U.S.A.

(*Received 30 June 1978*)

SUMMARY

1. Inactivation of delayed outward current was studied by voltage clamp of isolated neurone somata of the molluscs *Archidoris* and *Anisodoris*. During prolonged voltage clamp steps in normal artificial sea water delayed outward current rises to a peak and then declines to a non-zero steady-state. During repetitive clamp pulses at repetition rates slower than 2/sec, the amplitude of peak outward current in the second pulse is commonly less than the amplitude at the end of the preceding pulse, giving the impression of continued inactivation during the repolarized interval. We have termed this property cumulative inactivation.

2. Two components of delayed outward current were separated using tetraethyl ammonium ions (TEA) and cobalt ions (Co). External TEA blocks 90 % of a voltage and time dependent outward current termed K current (I_K). External Co blocks 85 % of a Ca activated delayed outward current termed Ca current (I_{Ca} does not inactivate during prolonged or repetitive voltage clamp pulses. I_K, however, inactivates during prolonged voltage clamp steps and shows cumulative inactivation during repetitive voltage clamp pulses.

3. Inactivation of I_K is voltage and time dependent and does not require influx of Ca ions.

4. As measured by a prepulse method, the onset of inactivation is characterized by a two time constant process. Fast inactivation occurs with a time course comparable to the rate of rise of outward current and can account for 90 % of total inactivation.

5. Recovery from inactivation is slow with a time constant approximately an order of magnitude slower than the onset of inactivation.

6. The current–voltage (I–V) curve for peak I_K can be N-shaped, with a region of negative slope resistance in the range of + 30 to + 80 mV. The I–V curve for steady-state I_K, however, shows little or no tendency to form a local maximum.

7. The pattern of delayed outward current varies considerably between cells. A major contributing factor to this variability appears to be the relative contributions of I_{Ca} and I_K to delayed outward current.

* Present address: Hopkins Marine Station, Stanford University, Pacific Grove, California 93950.

0022-3751/79/3840-0582 $01·50

INTRODUCTION

Inactivation of delayed outward current during voltage clamp depolarization has been reported in axonal as well as in somatic neuronal membrane (Hagiwara, Kusano & Saito, 1961; Ehrenstein & Gilbert, 1966; Connor & Stevens, 1971*a*; Lux & Eckert, 1974; Gola, 1974; Heyer & Lux, 1976*b*; Nakajima, 1966). In some molluscan central neurones the delayed outward current rises to an initial peak and then declines over a period of a few seconds during prolonged depolarization. Using K sensitive micro-electrodes positioned outside neurones of *Helix pomatia* Lux & Eckert (1974) observed a reduction in K efflux during the decrease in net outward current and concluded that K conductance activated by depolarization is subject to slow, time-dependent inactivation. A progressive frequency dependent decline in outward current amplitude occurs during repetitive depolarization. When two depolarizing pulses are repeated at frequencies near 1 Hz, the peak outward current during the second pulse is often less than the current at the end of the preceding pulse. This pattern of outward current gives the impression that the availability of outward current channels continues to decline during the repolarized interval. We have termed this feature cumulative inactivation.

Delayed outward currents in molluscan cells are composed of both voltage dependent and Ca dependent components (see Meech, 1978 for review). These components can be separated pharmacologically in nudibranch somata using tetraethyl ammonium ions (TEA) to block the voltage dependent component and cobalt ions to block Ca dependent current (Thompson, 1977). A series of voltage clamp studies was undertaken to localize the inactivation process to one of these two components using pharmacological methods to separate them, and to describe the properties of cumulative inactivation. The importance of cumulative inactivation of K current during repetitive action potentials is discussed in the following paper (Aldrich, Getting & Thompson, 1979). Neurone somata, isolated from the pleural and pedal ganglia of the nudibranchs *Anisodoris nobilis* and *Archidoris montereyensis* were studied. We found that inactivation of delayed outward current is restricted to a voltage dependent outward current termed I_K by Thompson (1977). Cumulative inactivation of I_K is voltage and time dependent and does not depend on the influx of Ca during depolarization.

METHODS

Preparation

Specimens of the dorid nudibranchs *Archidoris montereyensis* and *Anisodoris nobilis* were obtained from Pacific Biomarine Inc., Venice, California or collected in Monterey Bay, California, and were maintained in a recirculating sea-water system at 11 °C. Experiments were performed on large unidentified pleural ganglion neurones (about 200 μm diameter) and two identified neurones isolated from the pedal ganglia. These pedal neurones are the most prominent cell bodies on the dorsal surface of each pedal ganglion and are whitish in colour. We have termed these identified neurones pedal 5 and 6. The identified pedal cells were used to quantify the procedures used to separate and identify various components of delayed outward currents.

To facilitate the removal of muscle, connective tissue, and the inner epineural sheath overlying the neurone somata, the brain was removed from the animal and treated with a few grains of crystalline pronase (Sigma, grade B) for 2–4 min. Nerve cell bodies lie on the surface of the ganglion forming a rind with their axons projecting into an inner neuropil. In order to isolate

somata from their axons, sections of this rind containing three to four large neurones were carefully cut away from the neuropil using fine iris scissors (Connor, 1977). These sections were then pinned to the sylgard bottom of a lucite recording chamber and bathed in various saline solutions (Table 1) at 10 °C. The suitability of soma isolated by this method for voltage clamp studies has been well established (Connor, 1977). The isolated cells have normal resting potentials (−35 to −45 mV) and spike heights (70–90 mV). Measures of input resistance in the region of resting potential fall within the range of measurements for cells *in situ* (1–10 MΩ). Isolated cells are devoid of synaptic potentials, and under voltage clamp do not show axon-spike notches which indicate the presence of uncontrolled axonal membrane in intact cell preparations. The isolated cells we studied were either beating pace-makers, which fire repetitive action potentials at low frequency, or were silent at rest but fire repetitively in response to constant current stimulation.

Voltage clamp procedures

Neurones were impaled with two 3 M-KCl, bevelled micro-electrodes having resistances between 1 and 5 MΩ. Membrane potential was measured differentially between one of the intracellular electrodes and a third micro-electrode placed near the cell in the bath. The other intracellular electrode was connected to the output of a current clamp or voltage clamp amplifier similar to that used by Connor & Stevens (1971*a*), but modified to provide increased gain at very low frequencies (see Dionne & Stevens, 1975). The modification was necessary to preserve the closed-loop gain of the voltage clamp circuit during prolonged membrane currents.

Membrane current was measured by a virtual ground circuit (frequency response DC – 16 kHz) connected to the bath via an agar bridge and was filtered through a single-pole filter with a cut-frequency of 2 kHz. Membrane voltage settled in less than 200 μsec, however, the settling of capacitive currents required 0·5–1·0 msec due to the response characteristics of the virtual ground circuit and series resistance in the preparation. Permanent records of membrane voltage and current were recorded on a Brush 220 or 440 chart recorder (Gould, Inc.) with a full scale frequency response of 0–50 Hz, or filmed directly from an oscilloscope when the frequency response of the chart recorder was limiting.

A holding voltage of −40 mV was used in these experiments. This is the average resting potential (range −35 to −45 mV) for these cells both when isolated and *in situ*. In addition, at this holding voltage a transient outward current, termed I_A by Connor & Stevens (1971*b*), is inactivated. The voltage dependence of I_A inactivation was determined for each cell and only cells showing inactivation of I_A at −40 mV were included in this study.

Leakage currents were measured during a series of hyperpolarizing voltage pulses in the range −40 to −90 mV. Linear regression lines were fit to the voltage and current points and used to calculate the leakage current at depolarized voltages assuming ohmic behaviour. Leakage conductance ranged from 0·2 to 1·0 μS.

Sources of error in recorded current include the effects of uncompensated series resistance, and slow deterioration of the preparation. The magnitude of series resistance was approximated by applying a current step under current clamp conditions while recording the membrane voltage response. At the onset of the current step, recorded voltage first jumps instantaneously to a new value before beginning an exponential increase characteristic of a parallel circuit composed of membrane resistance and capacitance. The instantaneous jump in voltage is presumably developed across a resistance in series with the membrane resistance and its amplitude is assumed proportional to the magnitude of this series resistance. Estimates of series resistance range from 1 to 5 kΩ for these cells. No series resistance compensation was employed. We were careful to confine our measurements to cells and voltage ranges where membrane current did not exceed 1–2 μA. Assuming an average series resistance of 2 kΩ; the estimated error in recorded voltage falls in the range of 2–4 mV at the largest currents. Since outward currents in these dorid neurones show marked inactivation, the effect of uncompensated series resistance is to underestimate the degree of inactivation.

Over the time course of a typical experiment (1–3 h), the peak amplitude of outward current for a given voltage pulse sometimes showed a progressive decline or run-down. The reason for this is not clear. To control for run-down, test and control voltage pulses were alternated at 2 min intervals. The amplitude of the outward current during the test pulse was corrected assuming linear run-down between control pulses. Data from cells showing greater than 20% run-down over the entire time course of an experiment was rejected. An additional source of

systematic error is drift in the voltage measuring electrode. Any experiment showing greater than 5 mV drift was rejected.

The composition of the various saline solutions is shown in Table 1. TEA-saline was made by substituting TEA-Cl (Eastman Kodak, Co.) for equimolar amounts of NaCl yielding a final TEA concentration of 100 mM. Ca-free, Co substituted saline (Ca-free-Co) was made by omitting $CaCl_2$ and substituting equimolar amounts of $CoCl_2$ yielding a final Co concentration of 10 mM. CoCl stock solution was made fresh just before each experiment. Ca-free, Co saline with TEA

TABLE 1. Composition of saline solutions (mM)

	Normal ASW	TEA	Ca-free-Co	Ca-free-Co-TEA
NaCl	470	370	470	370
KCl	10	10	10	10
$CaCl_2$	10	10	0	0
$MgCl_2$	50	50	50	50
Tris	10	10	10	10
$CoCl_2$	0	0	10	10
TEA-Cl	0	100	0	100

(Ca-free-Co-TEA) was made by the dual equimolar substitution of 10 mM-$CoCl_2$ for $CaCl_2$ and 100 mM-TEA for NaCl. All salines were buffered to pH 7·6–7·8 at 10 °C by 10 mM-Tris-HCl (Sigma Chemical Co.). All experiments were performed at 10 °C. To avoid temperature transients, salines were maintained at 10 °C before perfusion into the experimental chamber. A minimum of five bath volumes was perfused for each solution change.

RESULTS

Outward current in dorid neurone somata

An example of membrane currents recorded in normal artificial sea water during a 4·3 sec voltage clamp step to + 10 mV is shown in Fig. 1*A*. After an initial inward current transient, membrane current becomes outward rising rapidly to a peak and then declining slowly to a stead-state value. The ratio of stead-state to peak outward current depends upon membrane voltage and differs among cells. During repetitive clamp steps at a frequency of 1/sec, peak inward current changes little. Peak outward current amplitude, however, declines progressively approaching a stead-state value by the tenth pulse (Fig. 1*B*). During the approach to stead-state, the peak outward current amplitude during each depolarization is less than the minimum outward current at the end of the previous pulse (dashed line, Fig. 1*B*). In addition, the time to peak becomes progressively longer until a stead-state rise-time is attained. The pattern of membrane currents during repetitive pulses gives the appearance of continued decline in the availability of outward current during the inter-pulse intervals. This is a characteristic feature of outward current in many molluscan neural somata and has been reported by Lux & Neher (1972), Gola (1974), Lux & Eckert (1974), and Heyer & Lux (1976*b*). We have termed this property cumulative inactivation. Experiments described below were undertaken to determine the membrane properties underlying cumulative inactivation.

Separation of outward currents

The outward current in nudibranch neurones may be separated into three distinct components (Thompson, 1977). One of these components, termed A-current (I_A) by

Connor & Stevens (1971*b*) is transient and is inactivated near the resting potential (Hagiwara & Saito, 1959; Connor & Stevens, 1971; Neher, 1971). Only cells showing inactivation of I_A at the hold voltage (-40 mV) were used in this study. The delayed outward currents activated by depolarization from -40 mV may be separated into two additional components on the basis of their different sensitivities to external

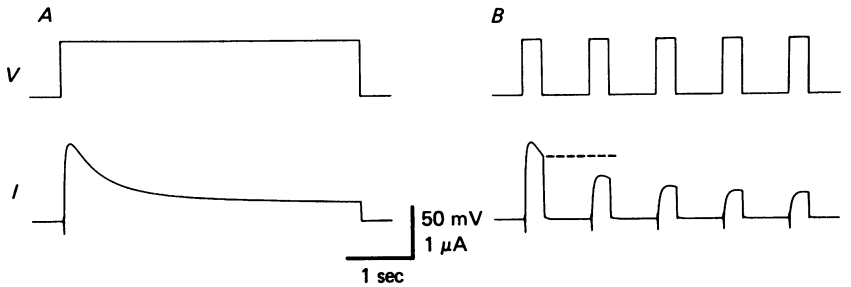

Fig. 1. Membrane currents in normal ASW. Membrane voltage (V) and resultant current (I) for an isolated unidentified pleural ganglion neurone are shown for a 4·3 sec clamp step to $+10$ mV from a holding potential of -40 mV (A) and for repetitive 300 msec pulses to $+10$ mV at a frequency of 1 Hz (B). During prolonged clamp steps (A), the outward current rises rapidly to a peak and then declines smoothly towards a non-zero steady-state level. During repetitive pulses (B) the peak amplitude of delayed outward current declines progressively for each successive pulse. Note that in B the peak current on each pulse is less than the minimum outward current at the end of the preceding pulse. This is particularly noticeable for the second pulse in B where the dotted line shows the minimum level of the current at the end of the first pulse. In addition, the time-to-peak for delay outward current increases during repetitive pulses. The time-to-peak for the first pulse in B is 100 msec while that for fifth pulse is 200 msec.

TEA ions and Co ions (Thompson, 1977). One component of delayed outward current. I_K, is substantially blocked by TEA saline applied externally. Activation of I_K occurs in a voltage and time dependent fashion qualitatively similar to the gating of delayed K current in axons (Thompson, 1977). The second component of delayed outward current, termed C current (I_C) is blocked in Ca-free-Co saline but not substantially blocked by TEA saline. I_C is thought to be activated by an increase in intracellular Ca concentration subsequent to Ca influx during depolarization. It corresponds to the Ca dependent potassium current observed in other molluscan somata (Meech & Standen, 1975; Heyer & Lux, 1976*b*; Thompson, 1977). The block of I_C by external Co presumably results from the blocking action of Co ions on Ca influx (Hagiwara & Takahashi, 1967; Hagiwara, 1973; for review, see Reuter, 1973). These differences in sensitivity to TEA and Co ions were used to separated I_K and I_C in order to study the contribution of each to the net outward current patterns shown in Fig. 1. Experiments quantifying the separation of I_C and I_K were performed on the identified pedal neurones 5 and 6.

Characteristics of outward current in TEA

Membrane currents during a 4·5 sec pulse and during repetitive 500 msec pulses to $+10$ mV in normal artificial sea water are shown in Fig. 2*A* for pedal cell 5. In normal ASW, outward current rises rapidly to a peak and then decreases slowly.

During repetitive pulses the peak current declines progressively. In Fig. 2*B* the same voltage pulses were applied with the cell bathed in TEA saline. The outward current activates more slowly than in the sea water and continues to increase in amplitude during prolonged depolarizations. No decline in maximum amplitude is observed during repetitive voltage steps. The outward current in TEA for this cell is predominantly I_C. This conclusion is justified on the basis of quantitative experiments

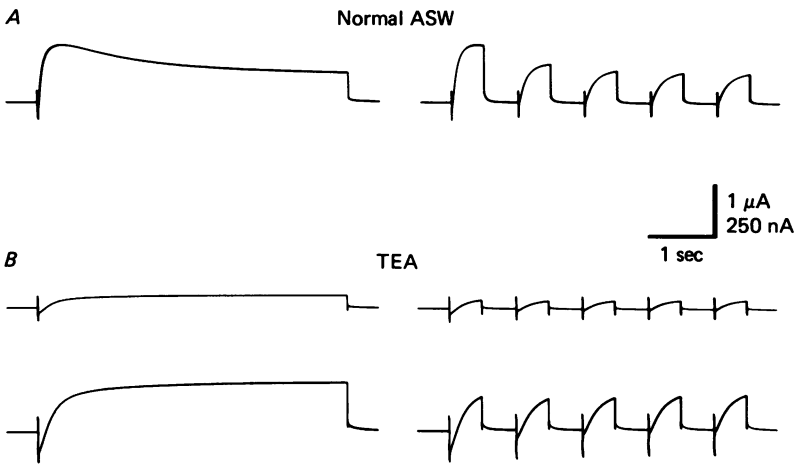

Fig. 2. Separation and characterization of I_C. In *A* the membrane currents recorded from an identified pedal ganglion cell 5 in normal ASW are shown for a 4·5 sec clamp step to +10 mV from a holding potential of −40 mV (left) and for repetitive 500 msec pulses to +10 mV at a frequency of 1 Hz (right). In *B*, the same pulse paradigmns were presented with the cell bathed in 100 mM-TEA saline. The membrane currents in *B* are shown at two gains; calibration bars are 1 μA for the upper traces and 250 nA for the lower traces. In TEA saline (*B*) a pronounced inward current is exposed during the initial 120 msec. The current then becomes outward and continues to increase throughout the duration of the clamp step. During repetitive pulses in TEA, the inward current becomes less pronounced while the peak outward current increases slightly from the first pulse (155 nA) to the fifth pulse (170 nA). For this cell, TEA saline blocks 87 % of the outward current at the time of peak outward current in normal ASW (*A*) and 29 % of the steady-state current. In normal ASW the steady-state to peak outward current ratio at −10 mV is 0·57 while the time-to-peak is 360 msec.

described below. These experiments indicate that cumulative inactivation is not a property of I_C.

Characteristics of outward current in Ca-free-Co saline

Membrane currents during long depolarization and during repetitive steps are shown for pedal cell 5 bathed in normal ASW and in Ca-free-Co saline (Fig. 3). In both solutions, outward current rises to a peak during a long depolarization and then declines slowly to a non-zero steady-state amplitude. During repetitive pulses, peak current declines progressively in amplitude accompanied by an increase in the time to peak. Outward current on depolarization from −40 mV in Ca-free-Co saline has been shown to be predominantly I_K (see below). I_K shows all of the features of cumulative inactivation (compare Fig. 3*A* to *B*). Since Ca influx is greatly reduced

under these conditions, this experiment also indicates that inactivation of I_K does not require Ca influx during depolarization.

Specificity of the separation

The effectiveness of using TEA and Ca-free-Co saline to separate I_K and I_C can be estimated from the analysis of tail currents which allows a temporal separation of the

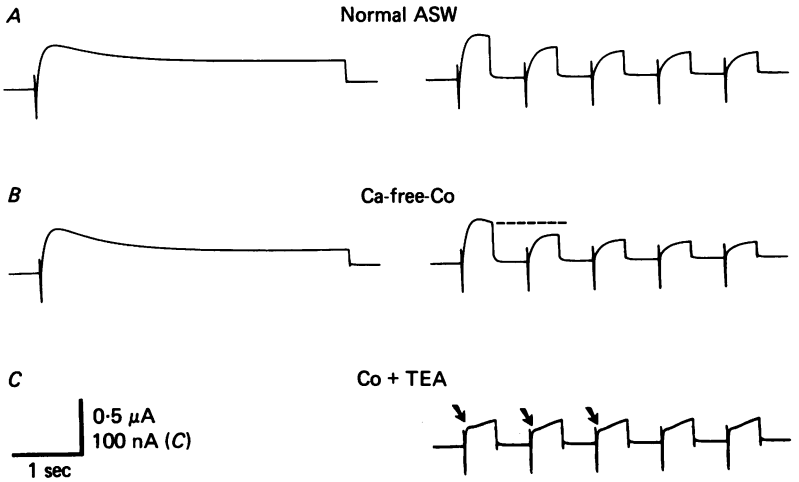

Fig. 3. Separation and characterization of I_K. In *A* the membrane currents for an identified pedal ganglion cell 5 in normal ASW is shown for a 4·5 sec clamp step to +10 mV from a holding potential of −40 mV (left) and for repetitive 500 msec pulses to +10 mV at a frequency of 1 Hz (right). In *B*, the same pulse paradigms were presented with the cell bathed in Ca-free-Co saline. The outward current patterns are nearly identical in these two solutions. Ca-free-Co saline results in a 2·5 % increase in peak outward current and a 29 % block of the steady-state current. During repetitive pulses the progressive decline in peak outward current is accentuated in Ca-free-Co saline. The difference between the peak amplitude of the first and second pulse in normal ASW (*A*) is 130 nA while in Ca-free-Co (*B*) it is 160 nA. Cumulative inactivation is indicated by the fact that the peak outward current on the second pulse in Ca-free-Co saline is less than the minimum current at the end of the first pulse (dashed line, *B*-right). In *C*, the same repetitive pulse paradigm was presented in Co+TEA saline which blocks 90 % of the outward current at +10 mV. In Co+TEA saline the outward current rises rapidly to a plateau (arrows) and then rises more slowly on a ramp. During repetitive pulses, the initial plateau (arrows) declines during successive pulses while the maximum outward current amplitude remains constant. We believe this current pattern reflects the incomplete block of both I_K by TEA and I_C by Ca-free-Co saline. For comparison to the cell of Fig. 2, this cell which is also an identified pedal ganglion cell 5 has a steady-state to peak ratio of 0·52 and a time-to-peak of 320 msec in normal ASW.

components. Upon repolarization to holding voltage (−40 mV) following a depolarizing step in normal ASW, a long outward tail current is observed.

A fast component of tail current which relaxes with a time constant of 100–300 msec is blocked by TEA and has been identified as I_K in a related nudibranch, *Tritonia* (Thompson, 1977). Slower components fall to one-half amplitude in about 10 sec and are blocked by Ca-free-Co saline. Slow components of tail current which are sensitive to Co ions have been previously identified as I_C (Thompson, 1977). In normal ASW,

I_C can be studied in isolation by measuring the amplitude of outward tail current at times greater than 1·2 sec after repolarization to hold potential. At this time (about four time constants) I_K should have declined to about 1% of its initial amplitude while I_C remains activated. The effect of TEA on I_C was studied by comparing tail currents in normal ASW to those in TEA saline. TEA blocks 10% (range 7–14%) of I_C measured 1·2 sec after a pulse. If residual I_K were present it would cause an over-estimate of the effect of TEA on I_C.

A similar analysis of tail currents 1·2 sec after repolarization in normal ASW and in Ca-free-Co saline indicates that external Co ions block 84% (range 79–92%) of I_C. In this case, if residual I_K were present it would result in an under-estimate of the affect of Ca-free-Co on I_C.

The combined application of TEA plus cobalt is shown in Fig. 3*C*. The amplitude of net outward current is much reduced under these conditions (compared Fig. 3*B* to *C*). The time course of residual outward current shows a rapid rise to an initial peak (arrows, Fig. 3*C*) followed by a slowly rising ramp. During repetitive depolarizations the initial peak current declines progressively while the current amplitude at the end of the pulse remains relatively constant. We interpret this current pattern to reflect incomplete block of both I_K and I_C in Ca-free-Co-TEA saline.

An estimate of the degree to which I_K is blocked by TEA can be made by comparing Fig. 3*C* with *B*. Comparison of the two current traces shows that addition of TEA to the already present Co results in 90% block of the early peak outward current. Contamination of peak current by residual I_C means that the measurement provides only a minimum estimate of the block of I_K by TEA.

Neither tail current analysis nor the combined application of TEA and Ca-free-Co saline can be used to accurately estimate the effect of external Co on I_K. This is because the relaxation of I_K and of rapid components of I_C overlap in time and because the relaxation of Ca tail current also occurs during this time. By comparing the outward current in normal ASW (Fig. 3*A*) with that in Ca-free-Co (Fig. 3*B*), however, it can be seen that the peak outward current amplitude in Ca-free-Co (410 nA) is larger than that in normal ASW (400 nA). The increase in outward current amplitude in Ca-free-Co saline is consistent with the notion that external Co ions block an inward Ca current and have minimal effect on I_K. A similar conclusion was reached by Thompson (1977) on other grounds. An accurate estimate of the effect of Co on I_K has not been made, however, and will only be possible with an independent method to block I_C.

The results of these separation experiments indicate that Ca-free-Co saline blocks approximately 84% of I_C while having minimal effect on I_K. TEA (100 mM), on the other hand, blocks approximately 90% of I_K with only a 10% reduction of I_C.

Inactivation of I_K

The decrease in net outward current in normal artificial sea water (shown in Figs. 1, 2*A*, 3*A*) is a result of decline in I_K. It is conceivable that the decline in I_K with prolonged or repetitive pulses could be due to factors other than a decrease in K conductance (G_K). A frequency dependent increase in inward current could sum with I_K during depolarization and cause a decline in recorded outward current. Also, accumulation of potassium in the extracellular space could cause a decrease in

driving force (Frankenhaeuser & Hodgkin, 1956; Eaton, 1972). We tested these two hypotheses in the following experiments.

Inward currents in molluscan neurones can be divided into two components (Geduldig & Greuner, 1970; Standen, 1975; Eckert & Lux, 1976; Connor, 1977;

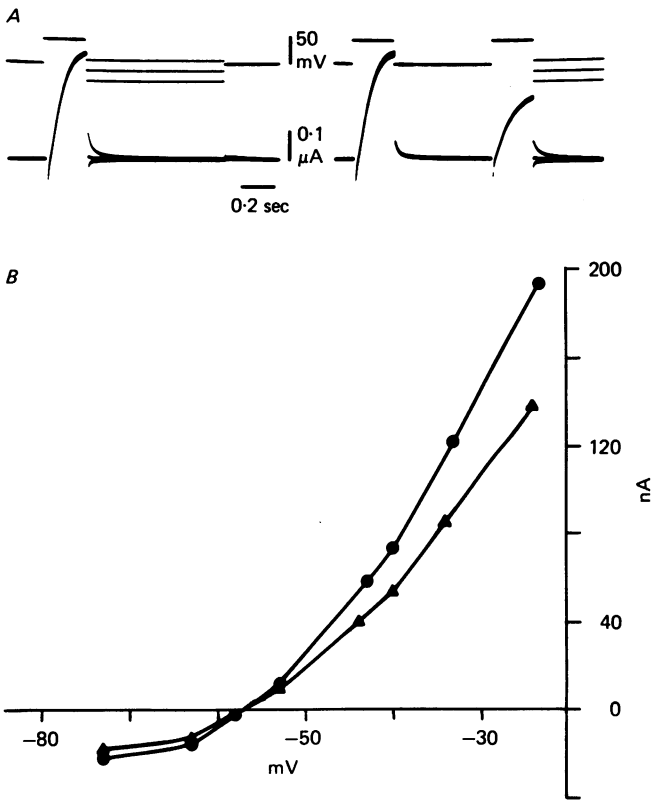

Fig. 4. Reversal potential for outward current tails in normal ASW. In *A*-left a 300 msec pulse to 0 mV is followed by a 1 sec repolarization pulse to various potentials. The tail currents at each repolarization potential was fit by a single exponential between 5 and 50 msec after repolarization. To construct the current–voltage plot of *B*, the extrapolated value of the tail at the time of repolarization is plotted (circles) as a function of the repolarization potential. Reversal potential is taken as the intersection with the zero current axis. In *A*-right the same procedure was applied after the second of two 300 msec conditioning pulses to 0 mV separated by 700 msec. The current–voltage relationship for tails after the second pulse is plotted in *B* (triangles). No significant shift in reversal potential is observed (−57 mV for a single pulse; −56 mV for two pulses) despite a 43% reduction in the maximum outward current during the second pulse.

Aldrich *et al.* 1979). One component rises rapidly and then inactivates during depolarization. It is sensitive to the external Na concentration and therefore corresponds in these aspects to the Na current in squid axon (Hodgkin & Huxley, 1952*a*). The second component rises more slowly and declines little during prolonged clamp steps (Lux & Eckert, 1974; Connor, 1977). It is observed in Na-free saline but not in Ca-free-Co saline, suggesting that it is a Ca current. Inward Ca currents have

been observed in a variety of molluscan cells (Adams & Gage, 1976; Connor, 1977; Eckert & Lux, 1976; Kostyuk, Krishtal & Doroshenko, 1975*a*; Kostyuk, Krishtal & Pidoplichko, 1975*b*; Aldrich *et al.* 1979). Under the conditions of our experiments, however, neither inward current contributes significantly to the decline in I_K during depolarization. The Na current inactivates rapidly within 100 msec at voltages between 0 and +10 mV and therefore does not significantly contaminate measures of peak or steady-state outward current amplitude. Ca current can be substantially reduced by application of Ca-free-Co saline without blocking the decline in outward current amplitude during depolarization (Fig. 3). The decrease in I_K, therefore, does not depend upon increased activation of inward currents. Similar conclusions were reached by Gola (1974) and Heyer & Lux (1976*b*).

The effect of extracellular K accumulation was assessed by measuring outward current reversal potential in normal artificial sea water on repolarization after a single pulse and after the second pulse of a pair. In the left pair of traces in Fig. 4, a single conditioning pulse to 0 mV for 300 msec from a holding voltage of −40 mV was repeated 3 times at 1 min intervals. After each conditioning pulse the cell was returned to a different repolarization voltage. The resulting tail currents were measured between 5 and 50 msec after repolarization and fitted by a negative exponential function using the method of least-squares. The tail current amplitude at zero time was estimated by extrapolation to the time of repolarization. The amplitude at zero-time is plotted against repolarization voltage to construct the current–voltage (I–V) curve for tail current after a single pulse (Fig. 4*B*).

The reversal potential for tail current is taken to be that voltage where the I–V curve crosses the voltage axis and is found to be −57 mV. Connor & Stevens (1971*a*) reported a similar value for delayed outward current reversal potential in Dorid neurones. The procedure was repeated in the right pair of traces, but this time the peak tail current after the second pulse of a two pulse pair (interpulse interval 700 msec) was measured at various voltages. Conditioning pulses and holding voltage were the same as before and the inter-trial interval was again 1 min. The I–V curve was constructed for the second pulse as before and the reversal potential was found to be −56·6 mV (Fig. 4*B*). Little shift in reversal potential was observed in spite of the fact that the peak outward current during the second pulse was only 57 % of that during the first. Shifts in outward current reversal potential do occur in these cells following prolonged, large depolarizations or during high-frequency repetitive pulses, indicating a tendency toward extracellular K accumulation. Such shifts do not usually occur at the low frequencies used in this study. These findings lead to the conclusions that the decline in outward current during low frequency repetitive depolarization does not result from a decrease in driving force due to potassium accumulation. The data support the hypothesis that the decline in outward current results from inactivation of K conductance (G_K). A similar conclusion was reached by Gola (1974) and Heyer & Lux (1976), but see Eaton (1972).

Voltage dependence of I_K inactivation

Inactivation of I_K was studied exclusively in Ca-free-Co saline. During prolonged clamp pulses, I_K rises to a peak and then declines to a stead-state level. It does not inactivate completely but the degree of inactivation depends upon pulse voltage.

The degree of inactivation was measured as the ratio of stead-state to peak I_K amplitude. This ratio is plotted against voltage in Fig. 5. Inactivation begins to increase sharply during depolarization from −40 mV and reaches a maximum at voltages between +10 to +20 mV. At maximal inactivation the ratio of steady state to peak I_K averages 0·26 (range 0·09–0·65 for twenty cells). With depolarizations above about +30 mV the ratio begins to increase, resulting in a U-shaped inactivation curve.

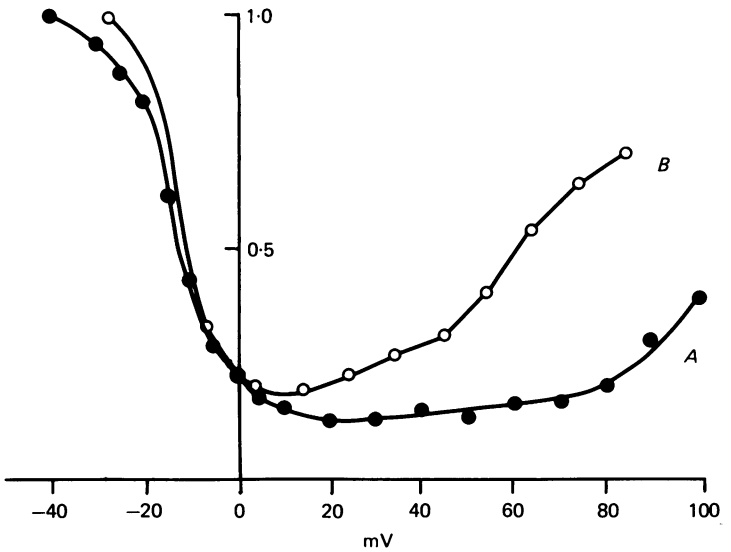

Fig. 5. Steady-state to peak current ratio. The steady-state to peak current ratio in Ca-free-Co saline is plotted as a function of membrane potential for the same two cells as shown in Fig. 8. The curves are U-shaped with a local minimum in the range of 0 to +20 mV. The decrease in inactivation (increase in steady-state to peak ratio) at voltages above +20 mV reflects the N-shaped nature of the peak current in Fig. 8 as compared to the monotonic increase in steady-state current (see text).

The voltage dependence of inactivation was also studied by a prepulse method. Fig. 6 shows the effect of depolarizing conditioning pulses on the peak amplitude of I_K during a later test pulse. Conditioning pulse amplitude was varied over the range −40 to +70 mV. Following a 1 sec inter-pulse interval (interval voltage −40 mV), a standard test pulse (+20 mV) for 300 msec was applied. An interpulse interval of one second was chosen to expose the maximum inactivation (see Fig. 12). The ratio of peak outward current amplitudes during the test pulse preceded with conditioning pulse (I) to the peak current amplitude in the absence of a conditioning pulse (I_0) is plotted as a function of conditioning pulse voltage in Fig. 6. The ratio I/I_0 decreases as conditioning voltage increases from −40 to about +30 mV indicating an increase in inactivation over this range. In some cells (cell *C*, Fig. 6), inactivation appears to saturate with increasing depolarization, while in others (cell *B*, Fig. 6) inactivation appears to decrease at pre-pulse voltages above +30 mV. Similar results have been reported for inactivation of total delayed outward current recorded in normal saline in *Helix* neurones (Eckert & Lux, 1977).

The effect of interpulse voltage on I_K inactivation is shown in Fig. 7. The pulse paradigm is shown in the insert. A test run consisted of a 250 msec pulse to +25 mV followed by a 2 sec interval of variable voltage and then another 250 msec pulse to +25 mV. The effect of interpulse voltages more positive than −40 mV is plotted in

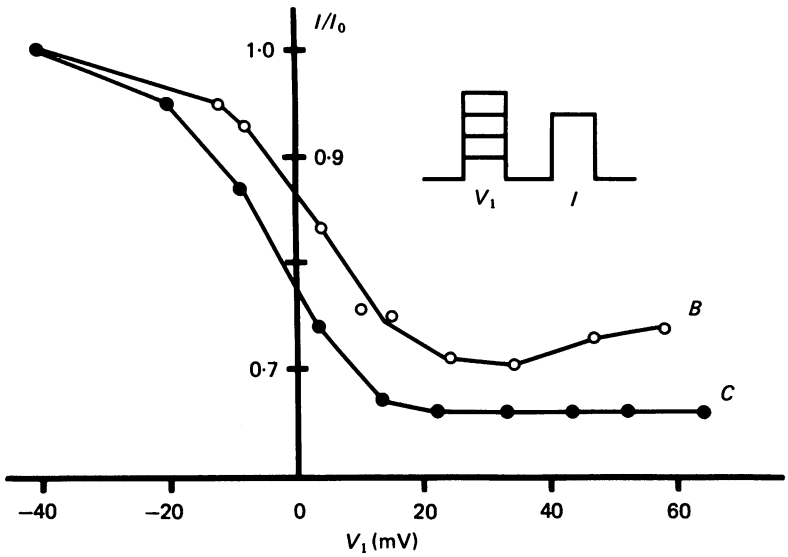

Fig. 6. Voltage dependence of inactivation determined by a prepulse method. The insert shows the pulse paradigm which consisted of a 200 msec prepulse to various voltages (V_1) followed 1 sec later by a constant test pulse to +20 mV for 300 msec. The ratio (I/I_0) of the peak current during the test pulse with (I) and in the absence of (I_0) the prepulse is plotted as a function of prepulse voltage. Curve B (open circles) is for cell B of Figs. 5 and 8. Bathing solution: Ca-free-Co saline. Prepulse and control stimuli were presented at 2 min intervals.

Fig. 7 (filled circles) as the ratio of the peak current during the second to that of the first pulse (I_2/I_1). For interpulse intervals below −40 mV, a different analysis procedure was necessary due to contaminating effects of A-current (I_A,) activation (Connor & Stephens, 1971*b*; Neher, 1971). Hyperpolarization below −45 mV removes I_A inactivation so that I_A will be activated by the second pulse to +25 mV.

We subtracted I_A from I_K using the following protocol (see insert Fig. 7). At each interpulse voltage below −40 mV, two different pulse paradigms were applied. The test paradigm consisted of the two pulses to +25 mV (I_1 and I_2) separated by a 2 sec interval. For the corresponding control, the first pulse to +25 mV was omitted but the 2 sec interpulse voltage was maintained. In the control paradigm, the outward current during the test pulse to +25 mV (I_3) consists of I_K plus I_A. To calculate the effects of interpulse hyperpolarization on I_K inactivation, I_2 was subtracted from I_3. In following this procedure, it is assumed that the reduction in peak current ($\Delta I = I_3 - I_2$) represents the loss in outward current due to inactivation of I_K caused by the first pulse. This assumption requires that the amplitude of I_A be the same for both the test and control paradigms. We chose an interpulse interval of 2 sec because this duration is at least 3 times the measured recovery time constant for I_A inactiva-

tion in the voltage range studied. Inactivation of I_A should, therefore, have reached the steady-state value appropriate to the interpulse voltage during the interval before the test pulse is applied.

The ratio of ΔI to I_1, where $\Delta I = I_3 - I_2$ and I_1 is the peak amplitude during the first pulse in the test paradigm, gives the fraction of I_K lost due to inactivation. To be

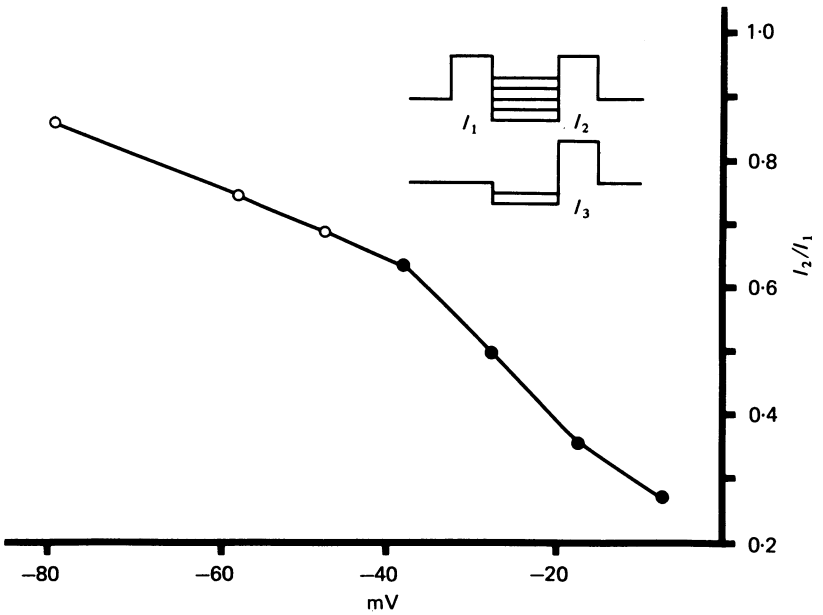

Fig. 7. Effect of interpulse voltage on inactivation. The pulse paradigms are shown in the insert. A test run consisted of two 250 msec pulses to +25 mV separated by a 2 sec interval of variable voltage. The effect of depolarizing interval voltages is plotted as the ratio (I_2/I_1) of peak outward currents as a function of the interval voltage (filled circles). To correct for I_A contamination at hyperpolarizing interval voltages, the ratio $1-(\Delta I/I_1)$, where $\Delta I = I_3 - I_2$ is plotted as a function of interval voltage (open circles). I_3 is the peak outward current during the test pulse in the absence of the first pulse to +25 mV. See text for details of the I_A subtraction. Bathing solution: Ca-free-Co saline.

consistent in the quantification of inactivation, values of $1-(\Delta I/I_1)$, which yield the proportion of I_K activated on the second pulse, are plotted as a function of interpulse voltage in Fig. 7 (open circles). Hyperpolarization below −40 mV causes a removal of inactivation. For depolarizing interpulse intervals, additional inactivation occurs during the interval and the increase follows closely the voltage dependence for inactivation shown in Fig. 5. We conclude that inactivation, once established, can be removed by hyperpolarization and increased by depolarization from the hold potential of −40 mV.

Current–voltage relation for I_K

To obtain the current–voltage relation (I–V curve) for I_K, 5–8 sec voltage clamp pulses were applied at a variety of membrane potentials in Ca-free-Co saline. Both peak and steady-state current amplitudes are plotted as a function of membrane

potential in Fig. 8 for two representative neurones. I_K does not activate significantly below -35 mV. At more positive voltages, peak I_K amplitude shows an N-shaped $I-V$ curve with a local maximum in the range of $+20$ to $+60$ mV. The amplitude of steady-state current, however, increases with membrane potential over the same voltage range with little or no tendency to form a local maximum. The ratio of steady-state to peak I_K yields the inactivation curve as a function of voltage shown in Fig. 5. The apparent recovery from inactivation with depolarization above $+30$ mV shown in Fig. 5 corresponds to the region of negative slope resistance in the $I-V$ curve of Fig. 8.

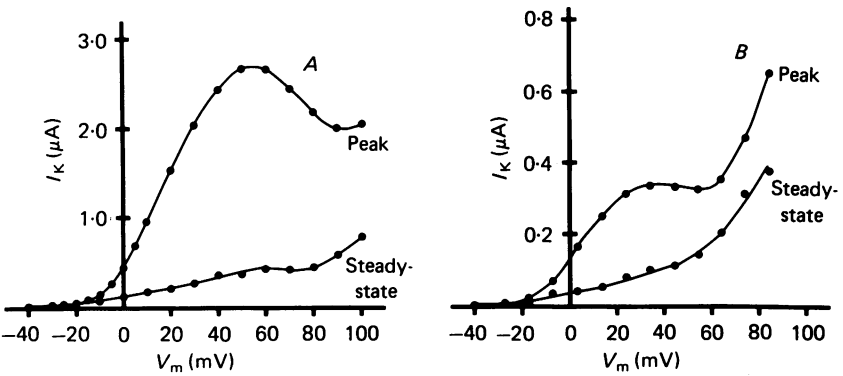

Fig. 8. Current–voltage curves for I_K in Ca-free-Co saline. The current–voltage ($I-V$) curves for peak and steady state outward currents are shown for two cells in Ca-free-Co saline. Peak I_K shows an N-shaped curve with a local maximum in the region of $+20$ to $+60$ mV. Steady state current, however, increases showing little (A) or no (B) tendency to form a local maximum. Since the steady state current increases, the N-shaped peak current curve cannot be attributed to an incomplete block of I_{Ca} by Ca-free-Co saline, but rather reflects the voltage-dependent properties of I_K activation and inactivation processes. A and B are for the corresponding cells of Fig. 5.

The $I-V$ curve for total delayed outward current measured at 300 msec in normal artificial sea water is also N-shaped in dorid neurones. In molluscan neurones in general, this N-shaped activation curve has been attributed to the properties of a Ca dependent outward current (I_C) (Meech & Standen, 1975; Heyer & Lux, 1976*a*; Thompson, 1977; Eckert & Tillotson, 1978). The results of Fig. 8 indicate that an N-shaped activation curve can be obtained when Ca influx is largely blocked in Ca-free-Co saline. The $I-V$ curve observed in Ca-free-Co saline might result from an incomplete block of I_C under these conditions, but this does not appear to be an adequate explanation. In Figs. 2 and 3 it is shown that the steady-state current in normal ASW is relatively more sensitive to block by Co ions than the peak current. Incomplete block of I_C should, therefore, show up as a prominent region of negative slope resistance in the $I-V$ curve for steady-state current in Co. This is not observed (Fig. 8). Our data indicate that the local maximum in the $I-V$ curve for peak I_K cannot be attributed solely to incomplete block of I_C.

Time dependence of I_K inactivation: onset time course:

The time course for the onset of inactivation was measured in a prepulse experiment. Prepulses of various durations to 0 mV were followed immediately by a 6 sec test pulse to + 20 mV (insert, Fig. 11). To control for run-down in I_K over long periods, test and control pulses were alternated at 2 min intervals and the sequence

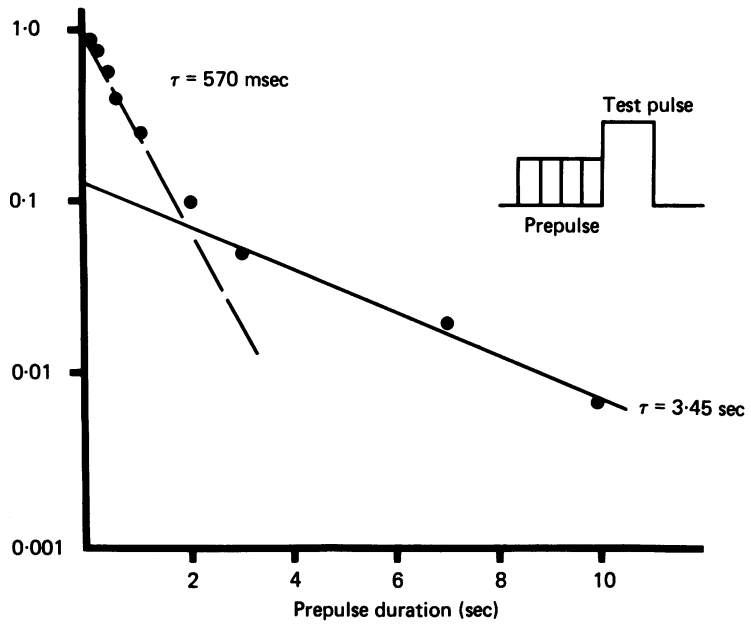

Fig. 9. Onset time course for inactivation as determined by a prepulse method. The pulse paradigm consisted of various duration prepulses to 0 mV followed immediately by a 6 sec test pulse to + 20 mV (insert). The ratio of I/I_0 where I is $I_{peak} - I_{steady\text{-}state}$ for the test pulse with a prepulse and I_0 is $I_{peak} - I_{steady\text{-}state}$ in the absence of a prepulse is plotted as a function of prepulse duration. The time course of inactivation can be approximated by the sum of two exponentials having time constants of 570 msec ($r^2 = 0{\cdot}98$) and 3·45 sec ($r^2 = 0{\cdot}99$) at 0 mV. The fast component of inactivation accounts for approximately 90 % of the total inactivation at 0 mV. Bathing solution: Ca-free-Co saline.

of prepulse durations was randomized. The test current (I) is measured as I_{peak} minus $I_{steady\text{-}state}$ for the test pulse at + 20 mV. The control current (I_0) was measured likewise as I_{peak} minus $I_{steady\text{-}state}$ in the absence of a prepulse. The log of the ratio of I to I_0 is plotted in Fig. 9 as a function of prepulse duration. Measured by this prepulse method, the onset of inactivation at 0 mV is fit well by the sum of two exponentials with time constants of 570 msec and 3·5 sec. More than 90 % of total inactivation occurs with the fast time constant. The rise time of I_K, measured as time-to-peak, was 180 msec at 0 mV for this cell. From Fig. 9 it can be seen that a 200 msec prepulse reduces the peak test current by 15 %, which corresponds to 30 % of the total inactivation. Thus the activation and inactivation processes have comparable time courses. This means that significant inactivation will have occurred

by the time of this peak, so that in the absence of any inactivation, the peak current would be significantly larger than observed.

Due to the long interstimulus intervals required for recovery from inactivation and the necessity to alternate control and test pulses, the prepulse technique has proven impractical to use in measuring the voltage-dependence of inactivation rate. A prepulse experiment over the voltage range of -40 to $+100$ mV would require over 6 hr, a period which is too long to obtain consistent results. An alternative technique

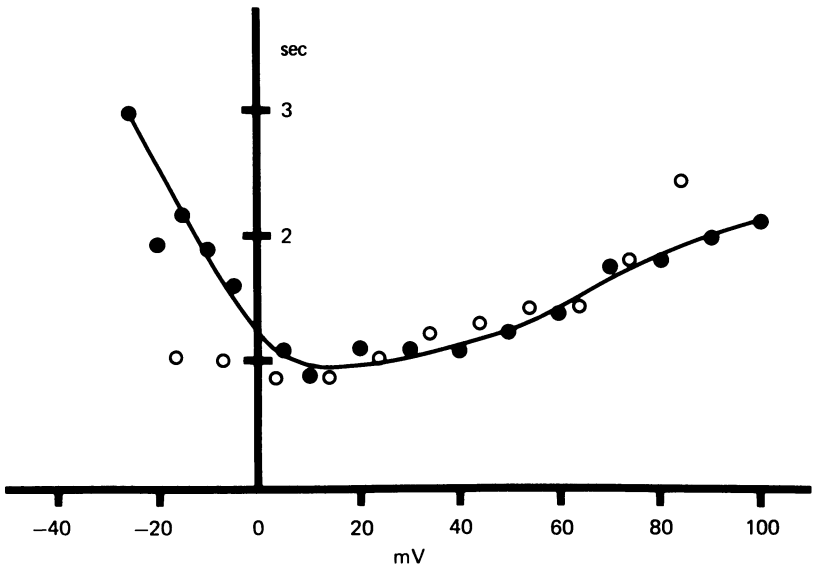

Fig. 10. Voltage dependence of inactivation time course. The inactivation time course was approximated by a single exponential fit to the decline in outward current during maintained voltage clamp steps at various voltages. The time constant for the single exponential fit is plotted as a function of step voltage for the same two cells as in Figs. 5 and 8 (filled circles, cell *A*; open circles, cell *B*). Bathing solution: Ca-free-Co saline.

was used to show the voltage dependence of inactivation time course during depolarization. This simplified method was used because it allows measurement of the inactivation time course at a large number of voltages within the experimental time constraints. The method is not entirely satisfactory because it does not allow resolution of the two time constants characterizing the inactivation process. Long pulses (6–8 sec) were applied at various voltages from -30 to $+100$ mV. The decline in I_K between 0·5 and 3 sec after the onset of depolarization was fit by a single exponential function by the method of least-squares. The decay time constant measured in this way is plotted in Fig. 10 as a function of voltage. The decay time constant decreases with depolarization and reaches a minimum between 0 and $+20$ mV. With depolarization above $+20$ mV, the time course of inactivation becomes progressively longer. These results are similar to those reported by Connor & Stevens (1971*a*) for cells bathed in normal ASW. It is not possible, however, to say from these experiments whether the voltage dependence of inactivation shown in Fig. 10 results from a parallel change in the kinetics of both fast and slow inactivation processes or from a change in the relative contributions of each process to the net level of inactivation at different

voltages. Additional experiments are required before we can discriminate between these possibilities.

Recovery time course

The time course of recovery from inactivation is shown in Fig. 11. Recovery was determined by measuring the ratio of peak current attained during two standard pulses to +10 mV applied at varying time intervals (Fig. 11*A*, insert). The voltage

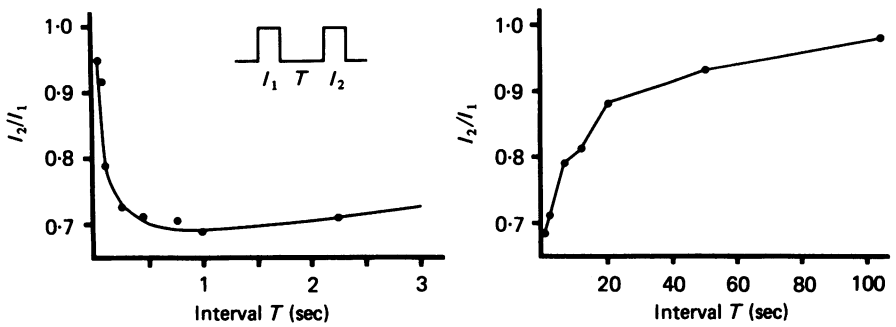

Fig. 11. Inactivation recovery time course at −40 mV. Recovery was determined by measuring the ratio of peak outward current (I_2/I_1) during two standard pulses to +10 mV separated by a variable interval T (insert). In *A*, the ratio of I_2/I_1 for one typical cell is shown for interpulse intervals below 3 sec. In *B* the ratio I_2/I_1 for the same cell is shown for longer intervals. The overall recovery curve is U-shaped with a minimal value between 1–2 sec for four cells. The recovery curve for times greater than 2 sec (*B*) can be fit well by a single exponential with time constants averaging 28 sec for four cells. Bathing solution: Ca-free-Co saline.

of the interpulse interval was −40 mV. After subtraction of leakage current, the ratio of peak current during the second pulse (I_2) to that of the first pulse (I_1) is plotted against interpulse interval in Fig. 11. At interpulse intervals shorter than 1 sec, inactivation increases with the interpulse interval (Fig. 11*A*). For intervals greater than one second recovery is observed (Fig. 11*B*). The over-all recovery curve is, therefore, U-shaped with maximal inactivation occurring approximately 1 sec after repolarization to hold voltage. The recovery curve for times greater than 2 sec can be fit well by a single exponential with a time constant averaging 28 sec (range 21–40 sec, four cells). Recovery from inactivation is, therefore, at least an order of magnitude slower than the onset of inactivation (Figs. 9 and 10). A similar U-shaped recovery curve has been reported for inactivation of total delayed outward current in normal saline for *Helix* neurones (Heyer & Lux, 1976; Eckert & Lux, 1977).

Voltage dependence of I_K onset time course

Since the faster component of I_K inactivation has a time course similar to that of the activation process (Fig. 9), it has not been possible to measure directly an activation time constant. As an alternative, the time to peak outward current is shown in Fig. 12 as a function of voltage. The time to peak reflects the relative rates of the activation and inactivation processes. For depolarizations above −20 mV, the time to

peak declines reaching a minimal value between + 30 to + 40 mV. At more depolarized voltages the time to peak increases resulting in a U-shaped curve.

Variability in delayed outward current among cells

Considerable variability in the pattern of outward currents during depolarization was observed between different neurone somata isolated from the pleural and pedal

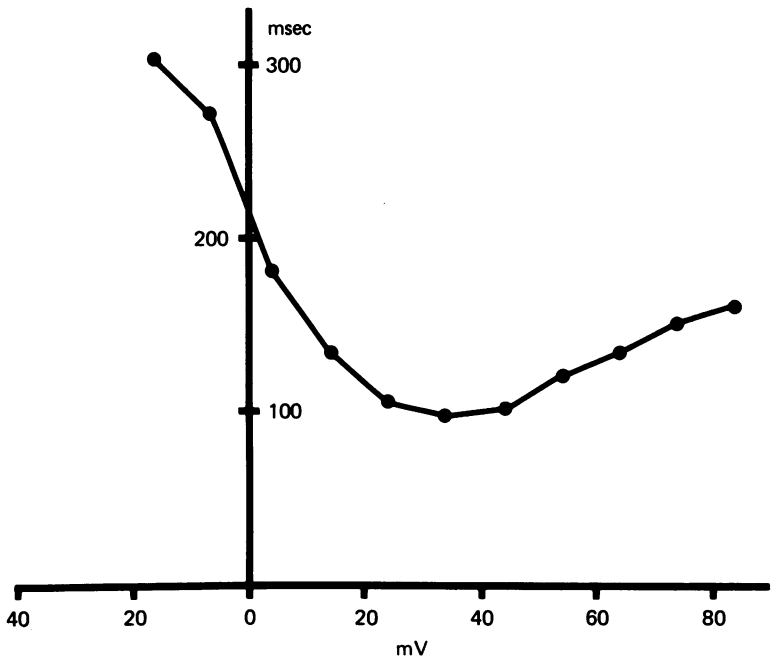

Fig. 12. Voltage dependence of I_K onset time course. The onset time course for I_K was measured as the time to peak current and is plotted as a function of membrane potential. Below − 20 mV little or no I_K is activated so that time-to-peak measures are not possible. With increasing depolarizations up to + 30 to + 40 mV time to peak decreases to a minimum. Above + 40 mV time to peak increases. Data presented is for cell *B* of Figs. 5 and 8.

ganglia. Cells differ in maximum degree of inactivation and time course of inactivation and recovery. The rise time for peak outward current at the onset of depolarization also differs as does the time course of tail currents on repolarization. A major source of variability apparently involves the relative contributions of I_K and I_C to total outward current in normal artificial sea water.

In Fig. 13 the membrane current in normal ASW is shown for two neurones representative of a continuum of outward current patterns. Membrane current for pedal cell 6 in response to a 2 sec voltage clamp pulse to + 10 mV is shown in Fig. 13*A*. Delayed outward current rises to a peak and then declines only to increase slowly again such that the current at the end of the voltage step is greater than the early peak current. In response to repetitive pulses at low frequency (1 Hz) the maximum outward current for each pulse declines progressively during the first few pulses but increases on later pulses. Our interpretation of this data is that the outward current

pattern results from the summation of contributions from I_K and I_C to the total outward current. I_K inactivates during prolonged depolarizations or repetitive pulses while I_C increases (see Figs. 2 and 3).

Membrane current for an unidentified pleural ganglion neurone is shown in Fig. 13*B*. In response to a 4·3 sec clamp pulse to +10 mV in normal ASW, the total delayed outward current rises to an early peak, and then declines monotonically to a low

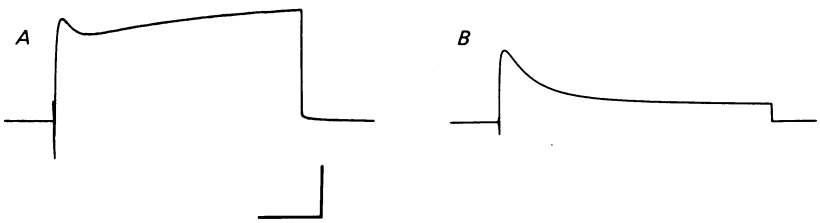

Fig. 13. Variability in outward currents in normal ASW between celltypes. *A*, membrane current recorded from pedal cell 6 during a 2 sec voltage clamp pulse to +10 mV. After an initial inward current transient, the outward current rises rapidly to an initial peak, then declines only to rise slowly again after a delay. This outward current pattern is typical of neurones with large contributions of both I_K and I_C to the total delayed current. *B*, membrane current recorded from an unidentified pleural neurone somata during a 4·3 sec voltage clamp pulse to +10 mV. For cells of this type, the delayed outward current rises to a peak and then declines smoothly to a steady-state value. The outward current pattern for cells of this type is affected little by substition of Ca-free-Co saline indicating that the delayed outward current is predominantly I_K. Calibrations: *A*, 0·5 μA and 2 sec; *B*, 1·0 μA and 1 sec.

steady-state amplitude. For cells of this type, Ca-free-Co saline has little or no effect on the early peak current and reduces the steady-state current by only 5%. On the other hand, TEA saline blocks up to 90% of both peak and steady-state current. These results suggest that the total outward currents consists almost entirely of I_K.

Due to incomplete block of I_K and I_C by TEA and Ca-free-Co respectively, the applicability of these pharmacological tools for the separation of current components depends upon the ratio of I_C to I_K amplitudes. If I_C/I_K is large, TEA can be used to study I_C since residual I_K will be comparatively small (e.g. cell A of Fig. 13). On the other hand, I_C cannot be isolated effectively in TEA saline when I_C/I_K is small; because residual I_K will contribute to the observed current. Similarly, I_K cannot be isolated by Ca-free-Co when I_C/I_K is large. In the experiments reported in this paper, I_K was studied in neurones of the type shown in Fig. 13*B* for which I_C/I_K is small and the outward current is dominated by I_K.

DISCUSSION

Pharmacological techniques were used to separate two components of delayed outward current and to localize inactivation to one of them. Based on our analysis, the outward currents recorded in Ca-free-Co saline are taken to be largely the voltage and time dependent current, I_K. During prolonged depolarization I_K shows inactivation which accumulates during repetitive clamp steps (Fig. 3). The Ca-activated outward current, I_C, recorded in TEA saline rises continuously during

prolonged depolarizations (Fig. 2). Summation of these two current components results in the pattern of delayed outward current recorded in normal ASW (Fig. 1, 2*A*, 3*A*). Considerable variability in the pattern of delayed outward currents was observed in different cells (Fig. 13). A large part of this variability evidently results from different relative contributions of I_C and I_K to total current. Care must be taken in the isolation and study of the various components due to incomplete block of I_K by TEA and of I_C in saline where Co is substituted for Ca. The incomplete block means that in applying these techniques to isolate currents one must select cells in which residual unblocked current is small relative to the current under study. This requires some knowledge of the relative contributions of I_C and I_K, i.e. the I_C/I_K ratio.

The study of I_C may be complicated by voltage or current dependent removal of the TEA block of I_K during depolarization (Herman & Gorman, 1978). The data shown in Figs. 2 and 13*A* suggest that such a process is not significant in our studies. In suitable cells, those in which I_C/I_K is high, a slow secondary growth in delayed outward current is observed during long depolarizations in normal artificial sea water (Fig. 13*A*). The time course of this secondary increase in outward current is similar to the slow increase in I_C observed in TEA saline (Fig. 2*B*). The similarity indicates that the recorded time course of I_C is probably not altered significantly by unblocking of I_K during depolarization.

Mechanism of inactivation

Heyer & Lux (1976) and Eckert & Lux (1977) proposed that in *Helix* neurones the accumulation of intracellular Ca contributes to inactivation of total delayed outward current. In dorid neurones this does not appear to be the case since we observe that inactivation is little affected in cells when calcium influx has been greatly reduced by Co blockade (Fig. 3*A* and *B*). These results do not address the question of possible involvement of Ca ions released from intracellular sites during depolarization. They do, however, indicate that neither Ca influx *per se* nor the substantial increase in internal free Ca ions resulting from influx is necessary for cumulative inactivation of I_K (see Plant, 1978). It does not appear that facilitation of inward Ca current proposed by Heyer & Lux (1976), Lux & Heyer (1977) and Eckert, Tillotson & Ridgway (1977) contributes significantly to the decline in delayed outward current in dorid neurones. The degree of inactivation is usually larger when Ca currents are substantially reduced by Co (Fig. 3). These conclusions are in agreement with those of Tillotson & Horn (1978) and Akaike, Lee & Brown (1978) who studied Ca currents in molluscan neurones and found no evidence for facilitation.

Inactivation of I_K appears to be a voltage and time dependent process. The time course of inactivation onset can be approximated by the sum of two exponential functions with time constants of approximately 570 msec and 3·4 sec at 0 mV (Fig. 9). On the other hand, the time-to-peak of I_K on depolarization to 0 mV averages 300 msec. The rate of activation and of the fast component of inactivation of I_K appear to be similar.

The data presented in this paper indicate that the kinetics of I_K are somewhat more complex than for axonal potassium currents (Hodgkin & Huxley, 1952*b*). *A*, inactivation is accumulated during repetitive voltage pulses. *B*, the time course

of inactivation onset as measured by the prepulse method (Fig. 9) is fit well by a sum of exponential functions. *C*, the recovery time course shows a U-shaped region at early times (Fig. 11). Any model proposed for inactivation of I_K must be able to account for these properties.

We suggest the following qualitative explanation for the mechanism of cumulative inactivation. Cumulative inactivation may result from the interaction of a fast inactivation at the onset of depolarization and the very slow recovery from inactivation. As stated above the time course for the onset of inactivation and the time-to-peak I_K are similar. This suggests that a considerable amount of conductance has been inactivated by the time of the peak current. After the peak, further inactivation occurs but largely by the slower inactivation process. Assuming that the amplitude of I_K is proportional to the number of open channels at a given time and voltage, the amplitude of I_K at the end of a voltage pulse reflects the number of non-inactivated channels at that time. If little or no recovery occurs during a short repolarized interval, then this is also the maximum number of available channels on a second depolarization to the same voltage. Fast inactivation during the second pulse will inactivate even more channels before the time of peak current. The peak current on the second depolarization will, therefore, be less than the current at the end of the preceding pulse. This hypothesis requires that little or no recovery occurs during the interpulse interval. The time constant for recovery from inactivation averages 28 sec (Fig. 11). Because of this long recovery time, channels which are inactivated during a voltage pulse are largely unavailable for reactivation by a second pulse applied within a few seconds.

The shape of the curve depicting recovery from inactivation deserves some comment (Fig. 11). It is of interest that the falling phase of the curve at early times corresponds to the time during which tail current after the first pulse is present (about 1 sec). It is possible that the presence of open channels during the tail current somehow decreases the probability of their inactivation during a second depolarization and maximum inactivation can only occur after the tails have relaxed to a steady state. Chandler & Meves (1970) observed a similar phenomenon in Na channels of squid axon perfused with fluoride ions. They attributed it to different kinetics and voltage dependencies of two separate transitions from inactivated to open states. A multi-state model for I_K inactivation may lead to a similar interpretation.

The correspondence between the early phase of the recovery curve and the presence of tail currents, suggests that the rate of inactivation may depend upon the state of the channel, for example, closed channels may be subject to inactivation by the rapid process whereas open channels may be inactivated by a slower process. This concept will account for the U-shaped nature of the recovery curve (Fig. 11) since open channels during the tail currents would not be subject to fast inactivation. This is a modification of the Hodgkin–Huxley formulation for sodium channel inactivation for which the rate of inactivation does not depend upon channel state, i.e. inactivation of open and closed channels is equally probably. There are, however, several examples of channel inactivation which are state dependent. Use-dependent 'inactivation' of Na channels has been reported for axons treated with local anaesthetics (Strichartz, 1973; Courtney, 1975) and in axonal potassium channels treated with various quaternary ammonium compounds (QA) injected internally

(Armstrong, 1969, 1971). Inactivation of I_K in molluscan somata is qualitatively similar to QA induced inactivation although the kinetics are much faster in squid axon. In particular, QA treated axons show a long recovery time course from inactivation especially if the compounds have large hydrophobic regions (Armstrong, 1971). Another similarity between I_K and QA treated axonal potassium currents is that membrane voltage during the interpulse interval effects the amount of inactivation between pulses. Depolarization during the interval increases inactivation of the second pulse whereas hyperpolarization during the interval removes inactivation (see Fig. 7). Armstrong (1969, 1971) has shown that at more hyperpolarized voltages, the probability of QA ions being dislodged from the channel by K ions entering from the outside of the channel is increased, leading to a removal of inactivation. Whether a similar mechanism underlies removal of I_K inactivation remains to be seen. A striking difference between I_K and QA treated K currents is that QA treated axons do not show accumulation of inactivation as shown in Figs. 1 and 3. There may, therefore, be fundamental mechanistic differences between the two phenomena.

The $I-V$ curve for peak I_K (Fig. 8) typically shows a region of negative slope resistance in the region of +30 to +80 mV. N-shaped activation curves have been reported for total delayed outward current in a variety of molluscs (Meech & Standen, 1975; Heyer & Lux, 1976; Eckert & Lux, 1977; Thompson, 1977), but in these cases the negative resistance region has been attributed to the properties of a Ca activated outward current (I_C). The $I-V$ curves of Fig. 8 were obtained from neurones bathed in Ca-free-Co saline which substantially reduces Ca influx and blocks about 85% of I_C. It is possible that part of the negative resistance regions results from an incomplete block of I_C but such a conclusion fails to explain the steady-state $I-V$ curve which shows little or no tendency to form a local maximum Incomplete block of I_C by Co should show up as a predominant region of negative resistance in the steady state rather than the peak $I-V$ curve. This was not observed (Fig. 8). In addition, since the activation of I_C is much slower than I_K (compare Figs. 2*B* to 3*B*), the relative contribution of I_K to the peak outward current is considerably larger than that of I_C. These considerations suggest that the negative resistance region of the $I-V$ curve for peak current in Ca-free-Co saline may reflect a voltage dependent property of I_K. One possible explanation for the negative resistance may be a differential voltage dependence for the inactivation and activation processes. Resolution of this hypothesis will require further experimentation to determine the relative voltage dependencies of the activation and inactivation processes. A second possibility is tha there are two populations of TEA-sensitive channels; for example one with inactivation and the other with slow or no inactivation. The shape of the $I-V$ curve may then reflect different voltage dependencies for the two types when measuring peak and steady-state values. We have, however, no evidence to support this hypothesis. In either case, the results indicate that the presence of a negative resistance in the delayed outward $I-V$ curve may not be sufficient evidence to demonstrate the presence of a Ca activated outward current.

This research was funded in part by N.I.H. research grant NS12529 to P. A. Getting, N.I.H. postdoctoral fellowship NS05234 to S. H. Thompson and N.I.H. training grants MH8304 and GM07181 to R. W. Aldrich.

REFERENCES

ADAMS, D. J. & GAGE, P. W. (1976). Gating currents associated with sodium and calcium currents in an *Aplysia* neurone. *Science, N.Y.* **192**, 783–784.

AKAIKE, N., LEE, K. S. & BROWN, A. M. (1978). The calcium current of *Helix* neurone. *J. gen. Physiol.* **71**, 509–531.

ALDRICH, R. W., GETTING, P. A. & THOMPSON, S. H. (1979). Mechanism of frequency-dependent broadening of molluscan neurone soma spikes. *J. Physiol.* **291**, 531–544.

ARMSTRONG, C. M. (1969). Inactivation of the potassium conductance and related phenomena caused by quaternary ammonium ion injection in squid axons. *J. gen. Physiol.* **54**, 553–575.

ARMSTRONG, C. M. (1971). Interaction of tetraethylammonium ion derivatives with the potassium channels of giant axons. *J. gen. Physiol.* **58**, 413–437.

CHANDLER, W. K. & MEVES, H. (1970). Evidence for two types of sodium conductance in axons perfused with sodium fluoride solution. *J. Physiol.* **211**, 653–678.

CONNOR, J. A. (1977). Time course separation of two inward currents in molluscan neurones. *Brain Res.* **119**, 487–492.

CONNOR, J. A. & STEVENS, C. F. (1971*a*). Inward and delayed outward membrane currents in isolated neural somata under voltage clamp. *J. Physiol.* **213**, 1–19.

CONNOR, J. A. & STEVENS, C. F. (1971*b*). Voltage clamp studies of a transient outward current in gastropod neural somata. *J. Physiol.* **213**, 21–30.

CONNOR, J. A. & STEVENS, C. F. (1971*c*). Prediction of repetitive firing behaviour from voltage clamp data on an isolated neurone soma. *J. Physiol.* **213**, 31–53.

COURTNEY, K. R. (1975). Mechanism of frequency-dependent inhibition of sodium currents in frog myelineated nerve by the Lidocaine derivative GEA968. *J. Pharmac. exp. Ther.* **194**, 225–226.

DIONNE, V. E. & STEVENS, C. F. (1975). Voltage dependence of agonist effectiveness at the frog neuromuscular junction: resolution of a paradox. *J. Physiol.* **251**, 245–270.

EATON, D. C. (1972). Potassium ion accumulation near a pace-making cell of *Aplysia*. *J. Physiol.* **224**, 421–440.

ECKERT, R. & LUX, H. D. (1976). A voltage-sensitive persistent calcium conductance in neuronal somata of *Helix*. *J. Physiol.* **254**, 129–151.

ECKERT, R. & LUX, H. D. (1977). Calcium-dependent depression of a late outward current in snail neurons. *Science, N.Y.* **197**, 472–475.

ECKERT, T. & TILLOTSON, D. (1978). Potassium activation associated with intraneuronal free calcium. *Science, N.Y.* **200**, 473–439.

ECKERT, T., TILLOTSON, D. & RIDGWAY, E. B. (1977). Voltage-dependent facilitation of Ca^{2+} entry in voltage-clamped aequorin-injected molluscan neuorns. *Proc. natn. Acad. Sci. U.S.A.* **74**, 1748–1752.

EHRENSTEIN, G. & GILBERT, D. L. (1966). Slow changes of potassium permeability in the squid giant axon. *Biophys. J.* **6**, 553–566.

FRANKENHAEUSER, B. & HODGKIN, A. L. (1956). The after-effects of impulses in the giant nerve fibres of *Loligo*. *J. Physiol.* **131**, 341–376.

GEDULDIG, D. & GRUENER, R. (1970). Voltage clamp of the *Aplysia* giant neurones: early sodium and calcium currents. *J. Physiol.* **211**, 217–244.

GOLA, M. (1974). Neurones a ondes-salves des mollusques, variations cycliques lentes des conductances ioniques. *Pflügers Arch.* **353**, 17–36.

HAGIWARA, S. (1973). Ca spike. *Adv. Biophys.* **4**, 71–102.

HAGIWARA, S. & TAKAHASHI, K. (1967). Surface density of calcium ions and calcium spikes in the barnacle fiber membrane. *J. gen. Physiol.* **50**, 583–601.

HAGIWARA, S., KUSANO, K., & SAITO, N. (1961). Membrane changes of *Onchidium* nerve cell in potassium-rich media. *J. Physiol.* **155**, 470–489.

HAGIWARA, S. & SAITO, N. (1959). Voltage-current relations in nerve cell membranes of *Onchidium verruculatum*. *J. Physiol.* **148**, 161–179.

HERMAN, A. & GORMAN, A. L. F. (1978). Blockage of the Ca^{2+} induced K^+ current by TEA in molluscan bursting pacemaker neurons. *Biophys. J.* **21**, 52a.

HEYER, C. B. & LUX, H. D. (1976*a*). Properties of a facilitating calcium current in pacemaker neurones of the snail, *Helix pomatia*. *J. Physiol.* **262**, 319–348.

HEYER, C. B. & LUX, H. D. (1976*b*). Control of the delayed outward potassium currents in bursting pace-maker neurones of the snail, *Helix pmatia*. *J. Physiol.* **262**, 349–382.

HODGKIN, A. L. & HUXLEY, A. F. (1952*a*). The components of membrane conductance in the giant axon of *Loligo*. *J. Physiol.* **116**, 473–496.

HODGKIN, A. L. & HUXLEY, A. F. (1952*b*). A quantitative description of membrane current and its application to conductance and excitation in nerve. *J. Physiol.* **117**, 500–544.

KOSTYUK, O., KRISHTAL, A. & DOROSHENKO, P. A. (1975*a*). Outward currents in isolated snail neurones. I. Inactivation kinetics. *Comp. Biochem. Physiol.* **51***C*, 259–263.

KOSTYUK, P. G., KRISHTAL, O. A. & PIDOPLICHKO, V. I. (1975*b*). Effect of internal fluoride and phosphate on membrane currents during intracellular dialysis of nerve cells. *Nature, Lond.* **257**, 691–693.

LUX, H. D. & ECKERT, R. (1974). Inferred slow inward current in snail neurones. *Nature, Lond.* **250**, 574–576.

LUX, H. D. & HEYER, C. B. (1977). An aequorin study of a facilitating calcium current in bursting pacemaker neurons of *Helix*. *Neuroscience* **2**, 585–592.

LUX, H. D. & WEBER, E. (1972). A g_k inactivation phenomenon in a nerve cell membrane. *Proc. IV int. biophys. Congr.* **3**, 222–223.

MEECH, R. W. (1978). Calcium-dependent potassium activation nervous tissues. *Annu. Rev. Biophys. & Bioeng.* **7**, 1–18.

MEECH, R. W. & STANDEN, N. B. (1975). Potassium activation in *Helix aspersa* neurones under voltage clamp; a component mediated by calcium influx. *J. Physiol.* **249**, 211–239.

NAKAJIMA, S. (1966). Analysis of K inactivation and TEA action in the supra-medullary cells of puffer. *J. gen. Physiol.* **49**, 629–640.

NAKAJIMA, S. & KUSANO, K. (1966). Behaviour of delayed current under voltage clamp in the supramedullary neurons of puffer. *J. gen. Physiol.* **49**, 613–628.

NEHER, E. (1971). Two fast transient current components during voltage clamp on snail neurons. *J. gen. Physiol.* **58**, 36–53.

NEHER, E. & LUX, H. D. (1971). Properties of somatic membrane patches of snail neurons under voltage clamp. *Pflügers Arch.* **322**, 35–38.

PLANT, R. E. (1978). The effects of calcium on bursting neurons: A modeling study. *Biophys. J.* **21**, 217–236.

REUTER, H. (1973). Divalent cations as charge carriers in excitable membranes. *Prog. Biophys. molec. Biol.* **26**, 1–44.

STANDEN, N. B. (1975). Voltage-clamp studies of the calcium inward current in an identified snail neurone: comparison with the sodium current. *J. Physiol.* **249**, 253–268.

STRICHARTZ, G. R. (1973). The inhibition of sodium currents in myelinated nerve by quaternary derivatives of lidocaine. *J. gen. Physiol.* **62**, 37–57.

THOMPSON, S. H. (1976). Membrane currents underlying bursting in molluscan pacemaker neurons. Ph.D. dissertation, University of Washington, Seattle, Wash.

THOMPSON, S. H. (1977). Three pharmacologically distinct potassium channels in molluscan neurones. *J. Physiol.* **265**, 465–488.

TILLOTSON, D. & HORN, R. (1978). Inactivation without facilitation of calcium conductance in caesium-loaded neurons of *Aplysia*. *Nature, Lond.* **273**, 312–314.